



# Characterization of defects introduced in Sb doped Ge by 3 keV Ar sputtering using deep level transient spectroscopy (DLTS) and Laplace-DLTS (LDLTS)

C. Nyamhere<sup>a,\*</sup>, A.G.M. Das<sup>b</sup>, F.D. Auret<sup>a</sup>, A. Chawanda<sup>a</sup>, W. Mtangi<sup>a</sup>, Q. Odendaal<sup>a</sup>, A. Carr<sup>a</sup>

<sup>a</sup> Department of Physics, University of Pretoria, Pretoria 0002, South Africa

<sup>b</sup> School of Information Technology, Monash South Africa, Roodepoort 1725, South Africa

## ARTICLE INFO

PACS:  
71.55.Cn  
72.20.Jv  
73.40.Ns

Keywords:  
Laplace-DLTS  
DLTS  
Defects  
Sputtering  
Germanium

## ABSTRACT

We have used deep level transient spectroscopy (DLTS), and Laplace-DLTS to investigate the defects created in antimony doped germanium (Ge) by sputtering with 3 keV Ar ions. Hole traps at  $E_V+0.09$  eV and  $E_V+0.31$  eV and an electron trap at  $E_C-0.38$  eV ( $E$ -center) were observed soon after the sputtering process. Room temperature annealing of the irradiated samples over a period of a month revealed a hole trap at  $E_V+0.26$  eV. Above room temperature annealing studies revealed new hole traps at  $E_V+0.27$  eV,  $E_V+0.30$  eV and  $E_V+0.40$  eV.

© 2009 Elsevier B.V. All rights reserved.

## 1. Introduction

Since the recent renewed interest in germanium (Ge) as a possible candidate for high performance complimentary metal-oxide-semiconductor (CMOS) devices because of its higher mobility at low electric fields [1], a lot of research work has been performed on the electrical properties of defects introduced during high-energy gamma, electron and proton irradiation [2–8]. The defects introduced by heavier particles than electrons have also been investigated, during electron beam deposition of Pt Schottky contact on n-Ge [2] and during the implantation of n-Ge by heavy ions [3]. It is generally believed that heavy low energy ions may create shallow complex defects when compared to electron irradiation and the resulting traps can influence the performance of devices. Sputtering is a widely used metal deposition and surface cleaning technique in microelectronics, and generally is associated with defect creation by low energy heavy ions. In this study trap levels introduced by sputtering with 3 keV energy Ar ions have been investigated. Defects introduced by low energy ions are important, particularly for shallow junction devices, as they will determine the reliability and performance of these devices.

## 2. Experimental procedure

We have used bulk grown n-type Ge with (111) crystal orientation, doped with antimony, (Sb) to a density of  $2.6 \times 10^{15} \text{ cm}^{-3}$  supplied by Umicore. Before metallization the samples of  $0.3 \text{ cm} \times 0.3 \text{ cm}$  in size were first degreased and then etched in a mixture of  $\text{H}_2\text{O}_2:\text{H}_2\text{O}$  (1:5) for 1 min. Immediately after cleaning they were placed in a vacuum chamber where AuSb (0.6% Sb), 130 nm thick, was deposited by resistive evaporation on their back surfaces as ohmic contacts. The samples were then annealed at  $350^\circ\text{C}$  in argon (Ar) for 10 min to minimize resistivity of the ohmic contacts. Prior to the Schottky contact fabrication, the samples were sputtered by 3 keV Ar ions of fluences,  $1 \times 10^{13} \text{ cm}^{-2}$  and  $1 \times 10^{14} \text{ cm}^{-2}$  using Auger electron spectroscopy (AES). The sputtering process resulted in approximately 500 Å, thick layer being removed. Immediately after sputtering, Pd contacts, 0.60 mm in diameter and 100 nm thick were deposited by vacuum resistive evaporation. After the contacts were formed, the samples were characterized by current–voltage ( $I$ – $V$ ) and capacitance–voltage ( $C$ – $V$ ) techniques at room temperature. The defects introduced were characterized by DLTS and Laplace-DLTS [4,5]. The ‘signatures’ of radiation induced defects (i.e. energy position  $E_T$  in band gap relative to the conduction band and valence band for the electron traps and hole traps, respectively, and their apparent capture cross section,  $\sigma_a$ ), were determined from Arrhenius plots of  $\log(T^2/e)$  vs.  $1000/T$ , where ‘ $e$ ’ is either the hole or electron emission rate, and  $T$  is the measured temperature in Kelvin scale.

\* Corresponding author. Tel.: +27 12 4203508; fax: +27 12 3625288.  
E-mail address: [cloud.nyamhere@up.ac.za](mailto:cloud.nyamhere@up.ac.za) (C. Nyamhere).

DLTS measurements were performed regularly over a period of 4 months to monitor defect stability and evolution at room temperature. To get more information on the defects introduced by Ar ions sputtering, the samples were then annealed isochronally for 20 min in Ar gas from room temperature up to 300 °C. After each and every annealing cycle, *I-V*, *C-V*, DLTS and LDLS measurements were performed.

### 3. Results and discussion

In this section we present the electronic properties of the defects created by Ar ion sputter damage. The annealing behavior of the defects is also discussed.

#### 3.1. Electron and hole traps

The DLTS spectra (Fig. 1) shows the finger prints of the hole traps recorded after 3 keV sputtering with Ar ions of fluence  $1 \times 10^{14} \text{ cm}^{-2}$ . Curve (a) shows the data collected immediately

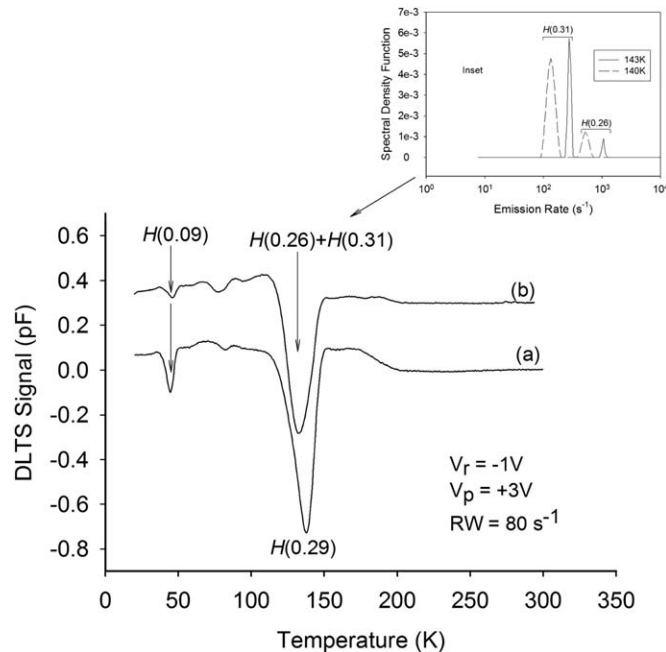


**Fig. 1.** The DLTS hole spectra after 3 keV Ar ions sputtering with a dose of  $1 \times 10^{14} \text{ cm}^{-2}$ , on n-Ge, (a) immediately after sputtering and (b) after room temperature annealing for a month. These spectra were recorded at a rate window (RW) of  $80 \text{ s}^{-1}$ , a quiescent reverse bias of  $V_r = -1 \text{ V}$  with a filling pulse  $V_p = +3 \text{ V}$  superimposed on the reverse bias and with a pulse width of 1 ms. Inset: The LDLS spectra of the  $H(0.26)$  and  $H(0.31)$  recorded at 140 K (dotted curve) and 143 K (solid curve) which appears as a single peak on the DLTS spectrum.

after irradiation and curve (b) shows the data after one month of room temperature storage. The DLTS spectra measured immediately after the sputtering reveals an electron trap level  $E(0.38)$  (spectrum not shown) and two hole traps  $H(0.09)$  and  $H(0.31)$  curve (a). In this nomenclature ‘E’ is the electron trap and ‘0.38’ is the position of the trap from the conduction band whereas ‘H’ is the hole trap and ‘0.09’ is the position of the trap relative to the valence band. After room temperature annealing for about a month a hole trap  $H(0.26)$  was observed. It should be noted that the un-sputtered Ge did not contain any defects in the detectable range limit, which is consistent with data in Refs. [6,7]. The defect ‘signatures’ for the radiation induced defects and those that evolved at room temperature were extracted from the Arrhenius plots, shown in Fig. 4 (filled circles) and the electron properties of these traps are summarized in Table 1. When compared with defects introduced in similar samples by 1 MeV electron irradiation [6–8], sputter deposition [9] and electron beam deposition [2],  $H(0.27)$  has a signature similar to  $H_{0.27}$  observed by Auret et al. [2].  $H(0.09)$ ,  $H(0.31)$  and  $E(0.38)$  have been assigned to the (+/0), (0/-), (-/-) charge states of the E-center, respectively [6–10]. The two levels  $H(0.26)$  and  $H(0.31)$  were observed as a single DLTS peak as shown in Fig. 1b but could clearly be separated by LDLS as depicted in the inset of Fig. 1. The LDLS peaks both shifted to higher emission rates with an increase in temperature, an indication that they are real defect peaks.

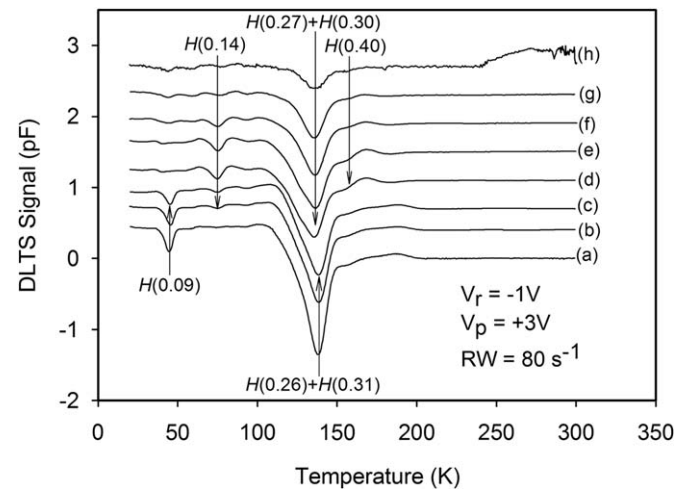


**Fig. 2.** The DLTS spectra showing defects created in n-Ge doped with Sb after sputtering with 3 keV Ar ions of dose  $1 \times 10^{14} \text{ cm}^{-2}$  (a) after room temperature annealing for a month, and after annealing at (b) 50 °C, (c) 150 °C, (d) 200 °C, (e) 225 °C, (f) 250 °C, (g) 275 °C and (h) 285 °C. The measurements were recorded at quiescent reverse bias,  $V_r = -1 \text{ V}$ , pulse voltage,  $V_p = +3 \text{ V}$ , pulse width of 1 ms and rate window (RW) of  $80 \text{ s}^{-1}$ .

**Table 1**  
The summary of electron properties of primary defects introduced by 3 keV Ar sputter damage in n-Ge and secondary defects introduced after thermal annealing.

Defect	$E_T$ (eV)	$\sigma_a$ ( $\text{cm}^2$ )	$T_{in}^a$ (°C)	$T_{out}^b$ (°C)	Similar defects/defect origin
$E(0.38)$	$E_C - 0.38$	$5.1 \times 10^{-14}$	RT	200	$E_{0.377}$ , $E_{0.37}$ , V-Sb (-/-) [2,3,6-10]
$H(0.09)$	$E_V + 0.09$	$7.8 \times 10^{-13}$	RT	200	$H_{0.09}$ , V-Sb (+/0) [10]
$H(0.14)$	$E_V + 0.14$	$1.3 \times 10^{-14}$	50	275	$H_{0.15}$ [2]
$H(0.26)$	$E_V + 0.26$	$1.8 \times 10^{-13}$	RT <sup>c</sup>	200	$H_{0.27}$ [2]
$H(0.27)$	$E_V + 0.27$	$8.1 \times 10^{-14}$	200	-	V, Sb, related?
$H(0.30)$	$E_V + 0.30$	$7.3 \times 10^{-14}$	200	-	V, Sb, related?
$H(0.31)$	$E_V + 0.31$	$3.3 \times 10^{-14}$	RT	200	$H_{0.30}$ , $H_{0.307}$ , V-Sb (0/-) [2,3,6-10]
$H(0.40)$	$E_V + 0.41$	$4.8 \times 10^{-11}$	200	-	V, Sb related?

<sup>a</sup> Temperature at which a defect anneals-in.

<sup>b</sup> Temperature at which a defect is removed.

<sup>c</sup> Annealed-in at room temperature after a month.

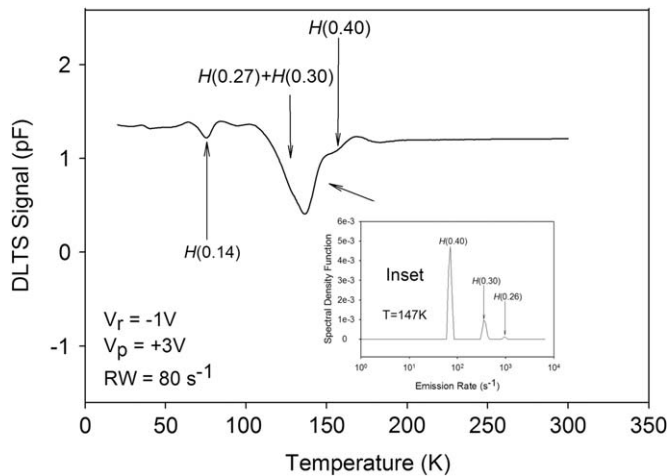


**Fig. 3.** The DLTS spectra for n-Ge doped with Sb after sputtering damage with 3 keV Ar ions with a dose of  $1 \times 10^{14} \text{ cm}^{-2}$  and annealed at 225 °C. The measurements were recorded at quiescent reverse bias  $V_r = -1 \text{ V}$ , pulse voltage  $V_p = +3 \text{ V}$ , pulse width of 1 ms and rate window (RW) of  $80 \text{ s}^{-1}$ . Inset: The LDLTS showing the peaks  $H(0.27)$ ,  $H(0.30)$  and  $H(0.40)$  recorded at 147 K which appear as a broad DLTS peak after annealing at 225 °C.

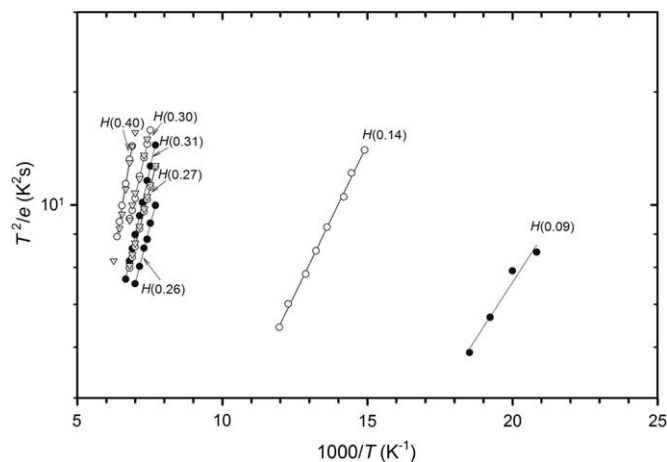


**Fig. 4.** The Arrhenius plots of the defects created in n-Ge after 3 keV sputtering with Ar ions with a dose of  $1 \times 10^{14} \text{ cm}^{-2}$  for as-sputtered and recorded after a month (filled circles), after annealing at 225 °C (open circles) and after annealing at 275 °C (open triangles).

### 3.2. Annealing behavior of the electron and hole traps

The annealing behavior of defects induced by 3 keV Ar ions sputtering on Ge is depicted in Fig. 2 and the electron properties extracted from the annealing graphs and Arrhenius plots depicted in Fig. 4 (open circles, after annealing at 225 °C) and (open triangles, after annealing at 275 °C) are summarized in Table 1. The hole traps  $H(0.09)$ ,  $H(0.26)$ ,  $H(0.31)$  and  $E(0.38)$  were stable up to 150 °C as shown in Fig. 2 curve(c) but  $H(0.31)$  was removed after annealing at 200 °C curve (d). The hole trap  $H(0.14)$  was introduced after annealing at 50 °C and was removed at 275 °C

whereas traps  $H(0.27)$ ,  $H(0.30)$  and  $H(0.40)$  are observed after annealing at 200 °C and were still present at the highest annealing temperature of 285 °C beyond which the diodes were too degrade for DLTS measurements. The defect levels  $H(0.27)$ ,  $H(0.30)$  and  $H(0.40)$  are clearly separated by LDLTS in Fig. 3 (inset) for a DLTS measurement at 225 °C. The Arrhenius plots in Fig. 4 clearly show that the pair  $H(0.27)$  and  $H(0.26)$  and the pair  $H(0.30)$  and  $H(0.31)$  are indeed different sets of defects. The peaks  $H(0.27)$ ,  $H(0.30)$  and  $H(0.40)$  are secondary defects observed after both the  $E$ -center and  $H(0.26)$  have been removed, strongly suggesting that these defects are formed when (a) V-Sb dissociates or (b) V-Sb diffuses and forms completely new higher order complex defects. Annealing studies of similar samples irradiated with electrons [7] did not reveal the same secondary defects suggesting that these complex defects are dependent on the mass and energy of the irradiating particles.

## 4. Summary and conclusions

The 3 keV Ar ion sputtering was shown to introduce primary traps,  $H(0.09)$ ,  $H(0.31)$ , and  $E(0.38)$ . After room temperature annealing for a month a trap  $H(0.26)$  was observed. These traps have also been observed in n-type Ge after electron beam deposition, sputter deposition and electron irradiation [2,6,8,9]. The annealing studies have further revealed new hole traps  $H(0.27)$ ,  $H(0.30)$  and  $H(0.40)$  which were all formed after the annealing of the  $E$ -center and  $H(0.26)$ , and they are probably V and/or Sb related higher order defects. More work in terms of defect models are required to identify these secondary defects.

## Acknowledgments

This work has been made possible by financial assistance from the South African National Research Foundation and Monash University, South Africa. The Laplace DLTS system software and hardware used in this research was received from L. Dobaczewski (Institute of Physics Polish Academy of Science) and A. R. Peaker (Centre for Electronic Materials Devices and Nanostructures, University of Manchester).

## References

- [1] R. Hull, J.C. Bean (Eds.), Germanium Silicon, Physics and Materials, Semiconductor and Semi-metals, vol. 56, Academic, San Diego, 1999.
- [2] F.D. Auret, W.E. Meyer, S. Coelho, M. Hayes, Appl. Phys. Lett. 88 (2006) 242110.
- [3] F.D. Auret, P.J. Janse van Rensburg, M. Hayes, J.M. Nel, W.E. Meyer, S. Decoster, V. Matias, A. Vantomme, Appl. Phys. Lett. 89 (2006) 152123.
- [4] L. Dobaczewski, P. Kaczor, I.D. Hawkins, A.R. Peaker, J. Appl. Phys. 76 (1994) 194.
- [5] L. Dobaczewski, A.R. Peaker, K.B. Nielsen, J. Appl. Phys. 96 (2004) 4689.
- [6] J. Fage-Pedersen, A. Nylandsted Larsen, A. Mesli, Phys. Rev. B 62 (2000) 10116.
- [7] C. Nyamhere, F.D. Auret, A.G.M. Das, A. Chawanda, Physica B 401–402 (2007) 499.
- [8] C. Nyamhere, M. Das, F.D. Auret, A. Chawanda, Phys. Stat. Sol. (C) 5 (2) (2008) 623.
- [9] F.D. Auret, S. Coelho, W.E. Meyer, C. Nyamhere, M. Hayes, J.M. Nel, J. Electron. Mater. 36 (2) (2007) 1604.
- [10] C.E. Lindberg, J. Lundsgaard Hansen, P. Bomholt, A. Mesli, K. Bonde-Nielsen, A. Nylandsted Larsen, Appl. Phys. Lett. 87 (2005) 172103.